



ORIGINAL ARTICLE

A new constitutive model for recycled aggregate concrete cylinders actively confined with post-tensioned metal straps

Ram Prasad Neupane^a, Thanongsak Imjai^{a*}, Reyes Garcia^b, U. Johnson Alengaram^c

^a School of Engineering and Technology, Walailak University, Nakhon Si Thammarat 80161, Thailand.

^b Civil Engineering Stream, School of Engineering, The University of Warwick, Coventry CV4 7AL, UK.

^c Department of Civil Engineering, Faculty of Engineering, Universiti Malaya, Kuala Lumpur 50603, Malaysia.

*Correspondence: thanongsak.im@wu.ac.th.

Abstract: The compressive strength of cylindrical columns of recycled aggregate concrete (RAC) is lower than that of equivalent normal concrete columns. Active confinement can recover some of such lower compressive strength, but limited research has examined the stress-strain behaviour of RAC cylinders with active confinement. This study proposes a new constitutive model for RAC cylinders actively confined with post-tensioned metal straps (PTMS). Using pneumatic tools, the PTMS technique involves applying a post-tensioning force to high-strength metal straps. RAC cylinders ($\varnothing 150 \times 300$ mm) with different confinement ratios ($\rho_v = 0, 0.35, 0.52, 0.80$ or 1.6) were subjected to axial compression tests to determine their maximum strength and axial strains. The RAC was produced using recycled concrete aggregate (RCA) as coarse aggregate, considering three compressive strengths: 15, 21 and 24 MPa. The test results indicate significant increases in strength and axial strains as the confinement ratio increased, with the strength increasing by 29% to 196%, and peak axial strains by 90% to 158% for ρ_v values of 0.35 and 1.6, respectively. Based on the test results and a regression analysis, a new stress-strain constitutive model is proposed to assess the effectiveness of the PTMS confinement on RAC. The results of this study promote the use of RAC in construction by demonstrating that the mechanical properties of RAC structural members can be effectively enhanced through the PTMS technique.

Keywords: Axial behaviour; active confinement; recycled aggregate concrete; ultimate strength; peak strain, stress-strain model

1 Introduction

Recycled aggregate concrete (RAC) is widely used in construction to promote the circular economy and sustainability of building materials. However, due to the inferior mechanical properties of RAC, it is mainly used in non-structural applications. Past studies show that the RAC has 10%–20% lower compressive, splitting, and flexural strengths compared to normal aggregate concrete (NAC) [1-2]. This is primarily due to the use of recycled concrete aggregate (RCA) in RAC, which contains large pores, adhered mortar residues, and surface cracks induced by the RCA's recovery process. This, in turn, increases the Poisson's ratio of RAC over that of NAC and reduces the modulus of elasticity by about 18% [3]. As a result, RAC elements subjected to compression experience larger lateral strains under a similar level of

000049-1



stress, thus reducing their mechanical performance. RAC structural elements also show a 6% to 24% lower performance in axial compression, shear and bonding behaviour compared to NAC counterparts [4-6]. Past studies also indicate significant inconsistencies in experimental results, primarily when high contents of RCA (close to 100% substitution of natural aggregates) are used in the RAC mix [7-10]. Whilst various treatments have been proposed to improve the properties of RCA, many of these are expensive or simply unfeasible at the large volumes required in concrete production. Therefore, the structural deficiencies of RAC tend to persist [4, 11-13], highlighting the need for strengthening to recover some of the structural strength. In particular, active confinement has been identified as a feasible alternative to enhance the comprehensive strength of RAC columns in a recent study [11].

Active confinement techniques with the use of Post-Tensioned Metal Straps (PTMS) have shown to improve the structural integrity, strength and ductility of NAC elements. Initial research by Frangou et al. [14] found that concrete cylinders confined with PTMS exhibited up to an 80% increase in strength compared to unconfined cylinders. Imjai et al. [15] reported an 8% increase in ultimate load capacity for PTMS-strengthened beams. According to Ma et al. [16], PTMS significantly increased the axial deformability (by 2.64 to 2.95 times) and the load capacity (by up to 313%) of pre-damaged plain concrete cylinders. Awang [17] expanded these findings to high-strength concrete columns, showing improvements correlated with increased confinement ratios. PTMS also significantly improved the load-bearing capacity of reinforced concrete (RC) columns and beams. For instance, through steel strapping tensioning techniques, Lee et al. [18] demonstrated increased concrete's load carrying capacity and ductility up to 17% and 22%, respectively. Similarly, Samadi et al. [19] showed that lap-spliced RC columns retrofitted with PTMS attained their theoretical yield strengths and a large 7% lateral drift displacement capacity, compared to 1.5% of the control specimen. Ma et al. [20] tested eccentrically loaded high-strength concrete columns and showed a 25% increase in ultimate load and a 41% increase in ductility over unconfined specimens. Overall, the PTMS approach has proven effective in improving the ductility and load-carrying capability of RC structures without considerably increasing their size or mass [21-22]. Moreover, PTMS offers advantages over traditional confining methods, such as rapid application and cost-effectiveness [23-24]. Whilst extensive research has explored the use of PTMS in improving the behaviour of normal and high-strength concrete columns, limited research has examined the effectiveness of PTMS in strengthening low-strength RC members [25-26]. Likewise, the effectiveness of active PTMS confinement on RAC elements remains unexplored [11].

Few studies have explored the effectiveness of lateral confinement on RAC elements. Some studies [27-29] highlighted significant improvements in recycled concrete strength and ductility. For example, Han et al. [29] discovered that RAC with a 33% replacement ratio, confined by three layers of polyethylene terephthalate-fibre reinforced polymer (PET-FRP), had a compressive strength 3.24 times higher and an ultimate axial strain 35.4 times larger than unconfined specimens. Previous works [17, 30-33] also suggested stress-strain models for NAC confined with highly ductile metal straps. However, given the distinct mechanical features of RAC, these models have to be tested for RAC. Moreover, to date there is no constitutive model for RAC confined with active PTMS, which provides a different confinement mechanism than passive materials and as such it can influence the stress-strain behaviour. Creating bespoke models for RAC confined with PTMS is critical since it may significantly increase compressive strength and ductility. Accordingly, this article seeks to address a knowledge gap by analysing current models and establishing new ones for RAC confined with PTMS, hence offering insights into sustainable concrete structures made from recycled materials.

This study proposes a new constitutive model for RAC cylinders actively confined with PTMS. RAC cylinders ($\varnothing 150 \times 300$ mm) with different confinement ratios ($\rho_v = 0, 0.35, 0.52, 0.80$ or 1.6) were subjected to axial compression until failure to determine their maximum strength and axial strains. The RAC was produced using RCA as coarse aggregate, considering three strengths: 15 MPa (M15), 21 MPa (M21) and 24 MPa (M24). Based on the test findings and regression analyses, a new stress-strain constitutive model is suggested to assess the effectiveness of PTMS confinement on RAC cylinders. This research's findings promote the utilisation of RAC in structural applications by demonstrating that the mechanical behaviour

of RAC columns can be effectively enhanced using the PTMS technique.

2 Experimental programme

2.1 RAC and NAC specimens

Forty-one RAC and thirty-three NAC cylinders were cast with a diameter of 150 mm and a height of 300 mm as part of the main tests. To obtain mechanical properties, nine cubic specimens of RAC and nine of NAC were cast, each with sides of 150 mm. Likewise, nine rectangular beams of RAC and NAC, each measuring 100 mm × 100 mm × 500 mm, were cast. **Figs. 1a-d** depicts the materials and equipment used to prepare the specimens, including high-ductile metal straps, clip locks, strain gauge insertion, sealing and strapping pneumatic tools, and the configuration of strapped cylinders. The detailed specifications are presented in **Appendix A**.

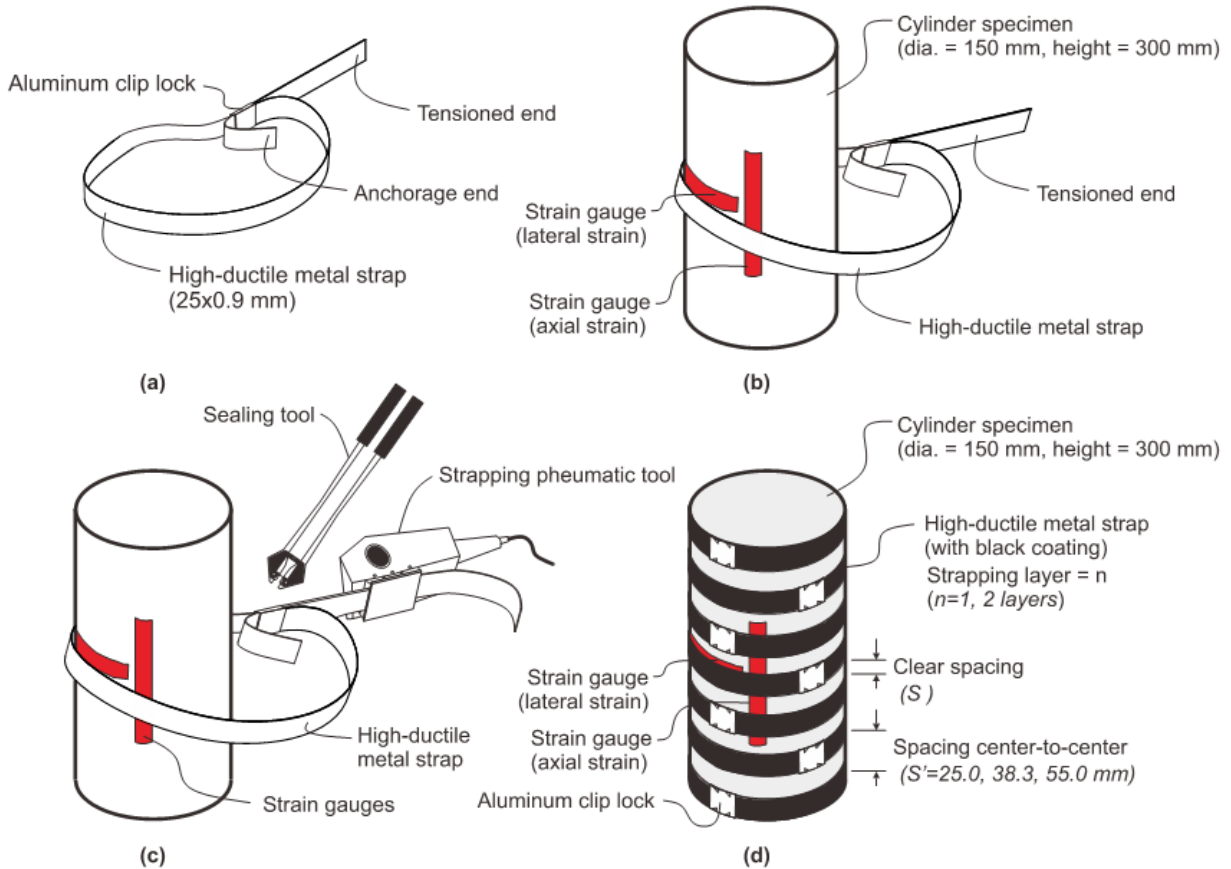


Fig. 1. Specimen details: (a) non-corrosive metal clip lock and high-ductile metal straps; (b) strain gauges on cylinders with metal straps; (c) sealing and strapping pneumatic tools used to secure the strap around cylinders; and (d) strap configuration and clear spacing.

2.2 Materials and properties

The concrete specimens for each of the three concrete strengths were cast in single batches, with the mix designs carried out according to ACI 211.1-91 [34]. Six concrete mixes with target 28-day compressive strengths of 15 MPa, 21 MPa, and 24 MPa were produced, including three NAC and three RAC mixes. The choice of such concrete strengths is consistent with international standards that define typical low- to normal-strength concretes for use in low-rise residential buildings and housing construction. For example, the German [35] and Italian [36] standards allow the use of strengths of up to 25 MPa. Japan [37] consents the use of strengths up to 36 MPa, whereas the UK [38] allows for strengths in a range of 20–40 MPa. The

selected strengths also permit investigate the effectiveness of the PTMS confinement over a range of different compressive strengths as those find in many typical structures of developing countries, where low-strength materials are often used. The six concrete mixes were produced with ordinary Portland cement. The coarse natural aggregates (NA) of the NAC mixes consisted of crushed stone sourced from a local quarry. Likewise, coarse RCA for the RAC mixes was produced from concrete waste crushed by an ad hoc machine [11]. After crushing, the RCA was sieved through a 20 mm sieve but ensuring that the material was retained on a 4.75 mm sieve. Locally available fine aggregate (size 0.15 - 4.75 mm) was used as sand. **Table 1** lists the basic properties of the aggregates used in this study. The maximum size of coarse aggregates is 20.2 mm for NA, 19.5 mm for RCA#2, and 10.3 mm for RCA#1. The bulk specific gravity (SSD) is 2.69, 2.31, and 2.48, respectively for such aggregates. The unit weights are 1576 kg/m³, 1305 kg/m³, and 1436 kg/m³. The water absorption rates are 0.39%, 6.02%, and 5.21%, respectively. The moisture content are 0.63%, 2.16%, and 2.21%. The impact values of the coarse aggregates are 10.23% for natural aggregates, 13.40% for RCA#2, and 12.45% for RCA#1, while the crushing values are 21.74%, 24.02%, and 20.24%, respectively. The residual mortar content is 31.52% for RCA#2 and 30.45% for RCA#1. The natural fine aggregate (NFA#1) has an upper size of 4.71 mm, a relative density of 2.64, a 1516 kg/m³ unit weight, an absorption value of 0.83% with 1.43% moisture content, and a fineness modulus of 2.68. The water-cement (w/c) ratio was maintained to achieve the desired workability (slump of 75 mm) in the concrete mixes. The average size of RCA is depicted in **Fig. 2a**. Likewise, the NA and RCA particle size distribution curves are shown in **Fig 2b**. **Fig 2b** shows that each curve approaches almost 100% at 19 mm. 50% of NA goes through the sieve at 10 mm, compared to 40% of RCA. Around 80% NA and 75% RCA pass through the 12 mm sieve. In general, NA passes more particles of bigger sizes than RCA. **Table 2** summarises the concrete mixes, including the actual w/c ratios for the different concretes.

Table 1. Physical and mechanical characteristics of aggregates

Properties	Coarse aggregates			Fine aggregate
	NA	RCA#2	RCA#1	NFA#1
Maximum size (mm)	20.2	19.5	2.36	4.71
Bulk specific gravity (SSD)	2.69	2.31	2.71	2.64
Unit weight (kg/m ³)	1576	1305	1450	1516
Water absorption (%)	0.39	6.02	2.79	0.83
Moisture (%)	0.63	1.16	2.56	1.43
Fineness modulus	-	-	1.90	2.68
Impact value (%)	10.23	13.40	-	-
Crushing value (%)	21.74	24.02	-	-
Residual mortar (%)	-	31.52	28.5	-

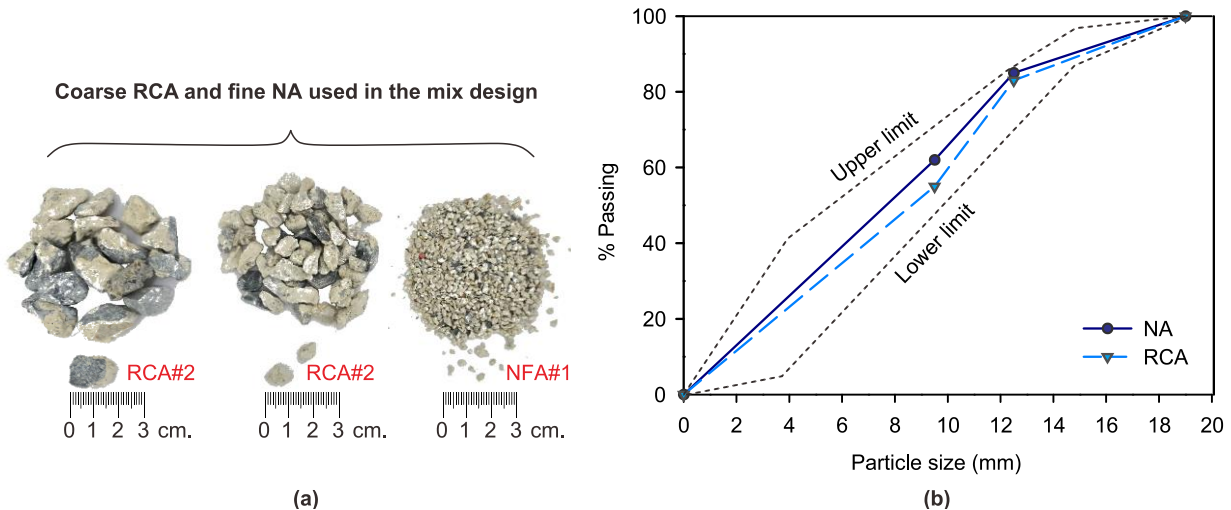


Fig. 2. (a) Typical RCA and NA aggregates used in this study, and (b) particle size distribution of NA and RCA.

Table 2. Mix designs in kg/m³ (slump = 75 mm)

Concrete grade	Concrete types	Cement	Fine aggregate	Coarse aggregate	Water	Actual w/c
M15	RAC	250.0	826.0	951.0	237.0	0.95
M15	NAC	250.0	747.0	1142.0	193.0	0.77
M21	RAC	294.0	788.0	951.0	237.0	0.81
M21	NAC	294.0	709.0	1142.0	193.0	0.66
M24	RAC	312.0	772.0	951.0	237.0	0.76
M24	NAC	312.0	694.0	1142.0	193.0	0.62

The average 28-day concrete strength was measured by testing cylindrical and cubical samples using BS EN 12390-3 [39]. A set of three cylinders was tested for indirect tensile splitting strength following BS EN 12390-6 [40]. The flexural strength was evaluated using four-point bending tests with three beams of each concrete type according to BS EN 12390-5 [41]. All specimens were cast and cured together in a controlled laboratory setting. The measured results of all tests are presented in **Table 3**. Three metal strap coupons with a cross-section of 0.9×25 mm were tested under direct stress to get the mechanical properties. The results show yield strength and strain values of 800 MPa and 0.06, respectively, and ultimate stress and strain values of 950 MPa and 0.014, respectively, with a modulus of elasticity of 200 GPa.

Table 3. Average 28-day mechanical properties of NAC and RAC hardened mixes

Compressive strength (MPa)		Splitting strength (MPa)		Flexural strength (MPa)		Remarks
NAC	RAC	NAC	RAC	NAC	RAC	
18.8	15.8	-	-	3.0	1.6	Cube/Prism
15.6	13.5	1.4	1.0	-	-	Cylinder
22.8	18.2	-	-	3.5	2.2	Cube/ Prism
19.9	15.7	1.7	1.3	-	-	Cylinder
29.6	23.9	-	-	4.8	2.9	Cubel/Prism
24.3	20.5	2.0	1.7	-	-	Cylinder

2.3 Metal strap installation

The confinement of the cylinders was implemented with varying spacing: 25 mm (for single and double layers), 38.30 mm, and 55 mm measured center to center, as shown in **Fig. 1**. The application of PTMS confining involved using a pneumatic strapping tool and clamping jaws, with the air pressure set at 8 bar (116 psi), a usual practical range for such tools. The applied prestress force was kept at up to 30% (240 MPa) of its yield stress. Studies have shown that the highest level of prestress for metal straps is up to 40% of their yield strength [42-45]. The effective volumetric confinement ratio (ρ_v), was calculated according to Eurocode 8 [46], whereas the *fib* Model Code 90 [47] was used to determine the confinement effectiveness coefficient over the cylinders' height. The samples are named based on their shape, compressive strength and strap spacing. For instance, specimen Cy-R24-1L-55-1 means 'Cy' = cylinder, 'M24' = strength of 24 MPa, 'R' = recycled aggregate, 'L' = layer, and '55' = PTMS spacing (S), and '1' is the first sample). **Appendix A** includes details of the calculated confinement parameters, including S' = centre-to-centre spacing of metal straps, n = number of layers of metal straps, ρ_v = volumetric confinement ratio, and f_{ie} = effective confining pressure. **Fig. 1** shows typical cylindrical specimens with different confinement ratios. The actual confined cylinders are presented in **Fig. 3**.

Due to stress relaxation in the metal clips and straps, post-tensioning methods such as the PTMS usually lose some tensioning force. Studies using similar components (e.g. Moghaddam et al. [42]) found no time-dependent reductions after two months. Imjai et al. [24] found 4%–15% prestress losses in single- and double-notched clips after 30 days. Similar tensioning force decreases were seen in lap-spliced beams confined with PTMS tested by Helal et al. [48-49]. These losses were mostly from the partial shearing off of the mild steel clip. In spite of these findings, the retention of most tensioning force (over 80%) suggests that post-tensioning losses are generally not problematic.

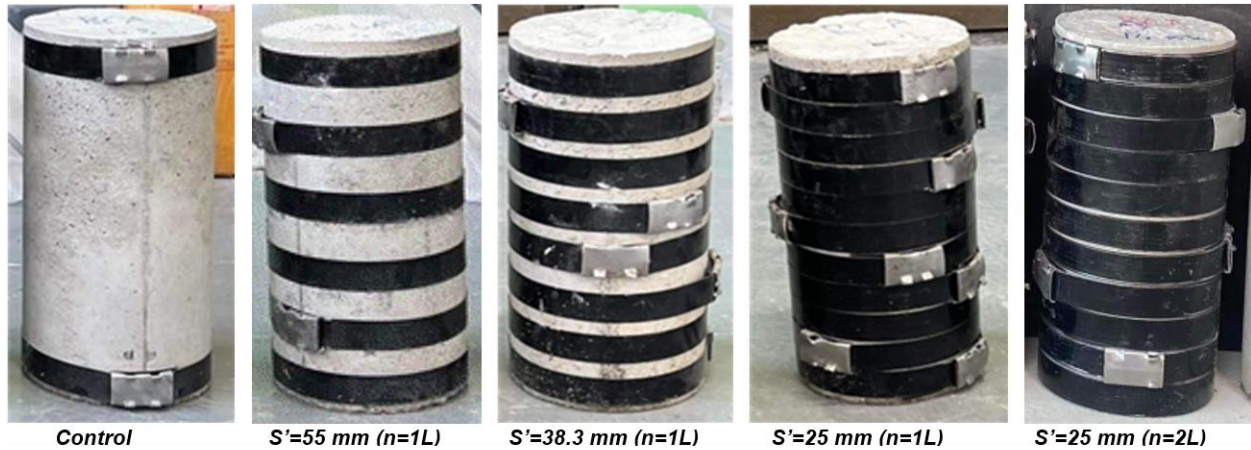


Fig. 3. Overview of concrete cylinders with different confinement configurations with different strap spacings (S') and number of layers of metal straps (n).

2.4 Test setup and instrumentation

Fig. 4a shows the arrangement for conducting axial compressive tests on cylindrical specimens using a universal testing machine with a 200 t capacity. Steel caps were placed at the top and base of the samples to ensure a uniform application of axial force. The load was applied using displacement control at a constant rate of 0.01 mm/s. Axial displacements of the cylinders were measured using two Linear Variable Displacement Transducers (LVDTs) with an accuracy of 0.001 mm and a gauge length of 50 mm, securely attached with sturdy supports. Strain gauges were utilised to capture strain data, while load and displacement data were logged at 5.0 Hz. The entire assembly is fixed on a solid floor with steel angles, making sure that the specimen is correctly aligned, as demonstrated in **Figs. 4a-b**. The actual experimental setup is shown in **Fig. 4b**.

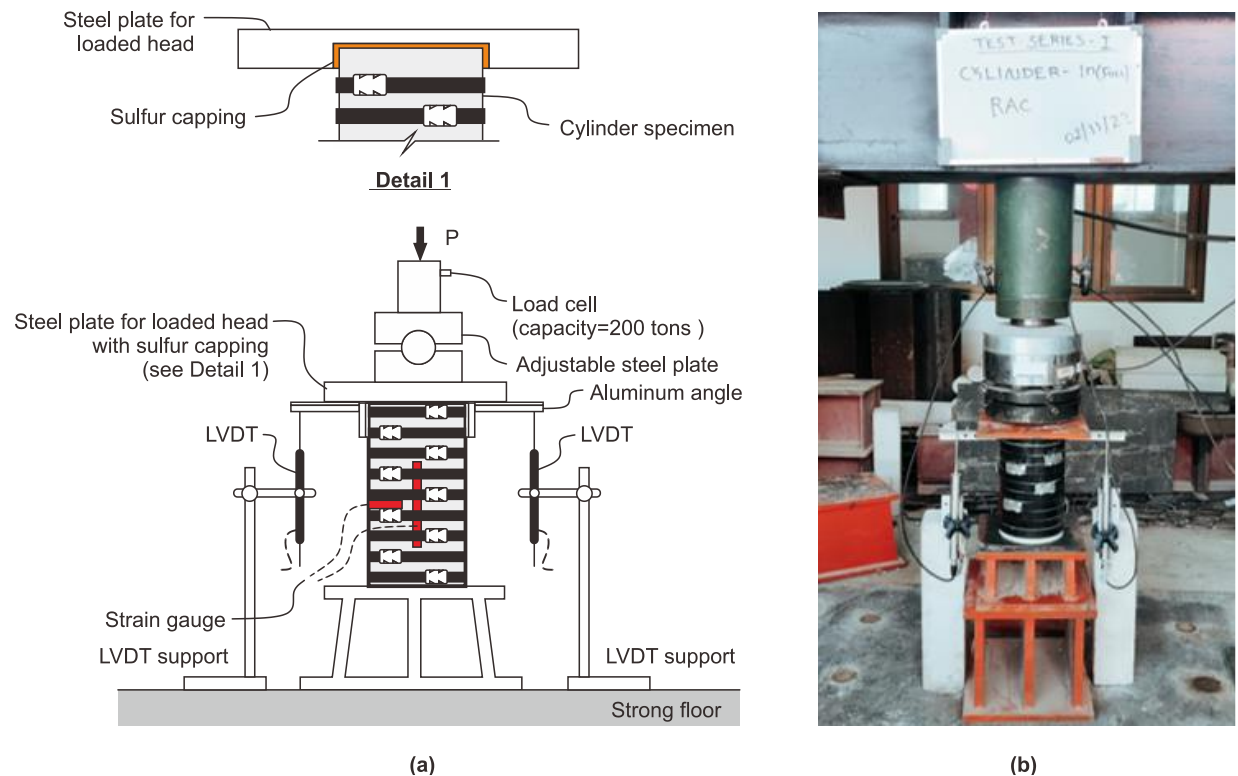


Fig. 4. Experimental setup: (a) instrumentation and steel caps, and (b) actual view of test set up.

3 Results and discussion

3.1 Capacity and failure mode

The amount of PTMS confinement (i.e. ρ_v) and the concrete's original strength all influenced the tested cylinders' behaviour. The experimental findings are depicted in **Table 4**, which displayed the combined effect of the above parameters on axial strains and strength. **Appendix B** summarises all test results. The outcomes indicate that external confinement notably enhances the ultimate strength and peak deformation of the PTMS confined cylinders. Overall, consistent compression behaviour was observed in the confined specimens' stress-strain curves and failure patterns, with better improvements at higher values of ρ_v .

Capacity enhancement: The unconfined compressive strength was 17.80 MPa for control RAC cylinders and 22.15 MPa for control NAC cylinders. The results from PTMS-confined RAC cylinders revealed that all such cylinders demonstrated significant enhancements in compressive strength (f_{cc}) and ultimate (peak) axial strain (ϵ_{cc}) proportional to their confinement ratios (ρ_v). Notably, strength gains compared with unconfined specimens were 29% at a ρ_v of 0.35, 50% at 0.52, 105% at 0.80, and 196% at 1.6. Likewise, the ultimate axial strains (ϵ_{cc}) exhibited increases of 90%, 94%, 98%, and 158%, respectively. In NAC cylinders with the same confinement ratios, the compressive strength increased by 14% at ρ_v of 0.35, 32% at 0.52, 78% at 0.80, and 161% at 1.6 compared to the control NAC cylindrical specimen. The ultimate axial strains in these cases increased by 88%, 104%, 120%, and 136%, underscoring the effectiveness of the confinement on both RAC and NAC cylinders.

Table 4. Test results of PTMS-confined cylinders

Specimen ID	P (kN)	δ (mm)	f_{co} or f_{cc}	$\frac{f_{cc}}{f_{co}}$	ϵ_{cc}	$\frac{\epsilon_{cc}}{\epsilon_{co}}$	f_{le}	ρ_v	Remarks
Cy-R24-c-1	321.2	1.53	17.80	-	0.005	-	-	0	Control
Cy-R24-1L55-1	414.1	2.90	22.95	+29%	0.009	+90%	0.73	0.35	
Cy-R24-1L38.30-1	481.9	2.97	26.71	+50%	0.009	+94%	1.64	0.52	
Cy-R24-1L25-1	657.7	3.01	36.45	+105%	0.009	+98%	3.84	0.80	
Cy-R24-2L25-1	952.2	3.93	52.77	+196%	0.012	+158%	15.36	1.60	
Cy-N24-c-1	399.6	1.15	22.15	-	0.004	-	-	0	Control
Cy-N24-1L55-1	456.2	2.16	25.28	+14%	0.008	+88%	0.73	0.35	
Cy-N24-1L38.30-1	527.1	2.35	29.21	+32%	0.007	+104%	1.64	0.52	
Cy-N24-1L25-1	711.5	2.53	39.43	+78%	0.009	+120%	3.84	0.80	
Cy-N24-2L25-1	1041.9	2.71	57.74	+161%	0.008	+136%	15.36	1.60	

Note: P is the maximum load, δ is the deformation at maximum load, f_{co} and f_{cc} are the ultimate stress for unconfined and confined specimens, ϵ_{cc} is the axial strain, f_{le} is the effective confinement pressure, ρ_v is the effective confinement ratio.

Figs. 5a-b depict the strengths and strains of PTMS-confined RAC and NAC cylinders for different confinement ratios (ρ_v). Normalisation is done over the experimental values obtained from the control cylinders. The results indicate significant strength and strain improvements in RAC and NAC cylinders. RAC shows higher normalised stress and strain increases, particularly if heavy confinement of $\rho_v = 1.6$ is used. The data confirm that higher ρ_v ratios improve performance (notably in RAC specimens), thus effectively increasing the PTMS-confined cylinders' load-carrying and deformation capacities.

Failure mode: **Fig. 6** compares the failure modes of unconfined control and PTMS-confined RAC cylinders. The unconfined control cylinders failed abruptly due to concrete crushing. Conversely, all PTMS-confined cylinders failed more gradually. This is due to the confining straps, which effectively controlled the lateral expansion of the RAC. For instance, the failure mode shifts from brittle to ductile at the higher confinement ratio of $\rho_v = 1.6$ in Cy-R24-2L25-1 (refer to **Fig. 6**). Cylinders with one strap layer demonstrated limited early cracking but failed explosively, thus suggesting that minimal confinement could not prevent excessive post-peak damage (see cylinder with $\rho_v = 0.35$ in **Fig. 6**). All PTMS-confined cylinders exhibited a pseudo-ductile behaviour, ultimately failing by concrete crushing combined with strap rupture at the mid-height of the cylinders.

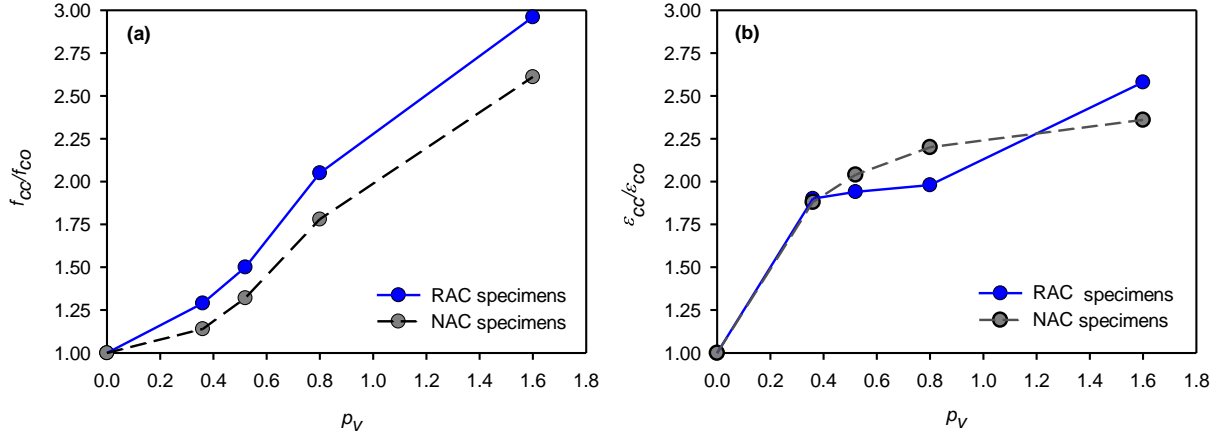


Fig. 5. Normalised (a) strength and (b) strains of PTMS-confined RAC and NAC cylinders for different confinement ratios (ρ_v).

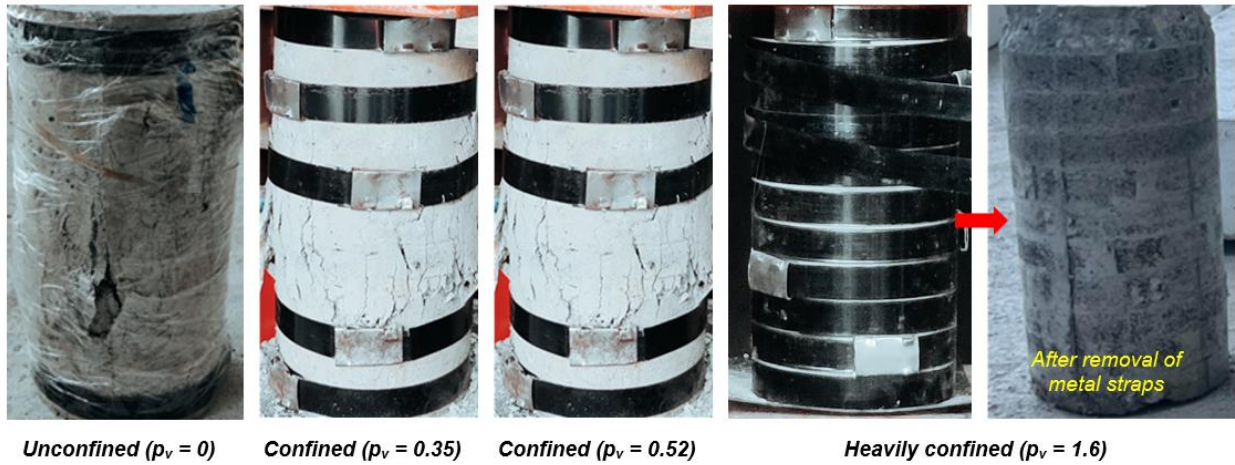


Fig. 6. Typical failure of cylinders according to confinement ratios.

3.2 Effect of RCA replacement

To evaluate the effect of coarse RCA replacement on the behaviour of unconfined and confined cylinders, a comparison was conducted between 0% and 100% replacement levels of NA with RCA across three different strengths: 15 MPa (M15), 21 MPa (M21) and 24 MPa (M24). The results, as detailed in **Table 3**, show that for the M15 grade, cylinders with 0% replacement exhibited higher compressive strength (15.7 MPa) than those with 100% replacement of RCA (13.5 MPa). In the M21 grade, NAC cylinders with no aggregate replacement had a compressive strength of 19.9 MPa, surpassing the 15.7 MPa recorded for 100% RCA. Similarly, in the M24 grade, cylinders with no aggregate replacement achieved a higher strength of 24.30 MPa compared to 20.53 MPa for those fully replaced with RCA.

Fig. 7 compares the normalised compressive strength with different RAC and NAC confined cylinder grades. The results show that RAC cylinders with 100% RCA replacement exhibited better confinement effectiveness, despite their low unconfined strengths. For M15, the PTMS-confined RAC cylinders surpassed the 0% RCA cylinders (denoted by NAC) by 19%, 8%, and 21% at strap spacings (S') of 55 mm, 38.30 mm, and 25.00 mm for single layers, respectively, but fell short by 16% at a strap spacing of 25.00 mm for double layers. For the M21 samples, PTMS-confined RAC cylinders had higher normalised strengths, with increases of +11%, +6%, +25% and 27% at the same level of confinement. For the same spacing and confinement layers, the M24 PTMS-confined RAC cylinders had higher strengths by +15%, +18%, +27%, and +35%, over the confined NAC cylinders. The results in **Fig. 7** suggest that the

effectiveness of confinement is influenced by the concrete's initial strength and the type of aggregate used. **Fig. 8** compares the experimental stresses and strains as a function of the PTMS confinement ratios in RAC and NAC cylinders. The results indicate a linear relationship linking the normalised axial stress and the normalised axial strain. It is also shown that higher confinement ratios led to higher enhancements in both strain and stress. **Fig. 8** also indicates that under heavily PTMS-confined conditions of $p_v=1.6$ ($S'=25.0$ mm-2L), the RAC cylinders had a normalised stress and strain increase of +35% and +22% compared to their NAC counterparts. This indicates that RAC and NAC react differently to the application of stress and strain. Overall, the outcomes show that increasing confinement improves the strength and deformation of both RAC and NAC cylinders, with better improvements in the RAC. The results also highlight the benefits of higher ρ_v values in enhancing the RAC cylinders' load-carrying and deformation capacities.

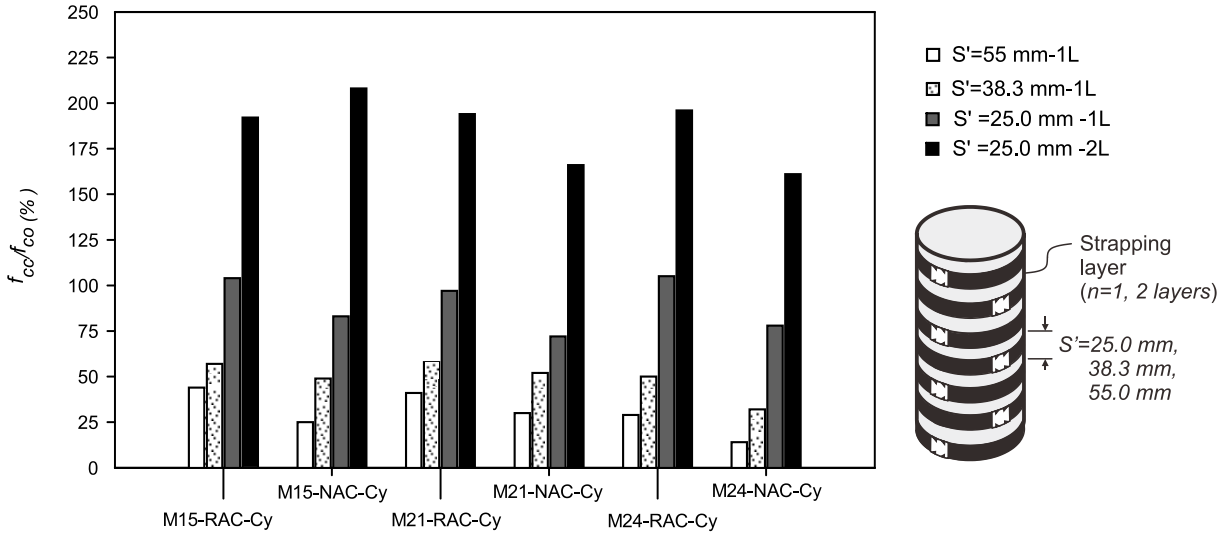


Fig. 7. Confinement effectiveness as the type of concrete (NAC vs RAC).

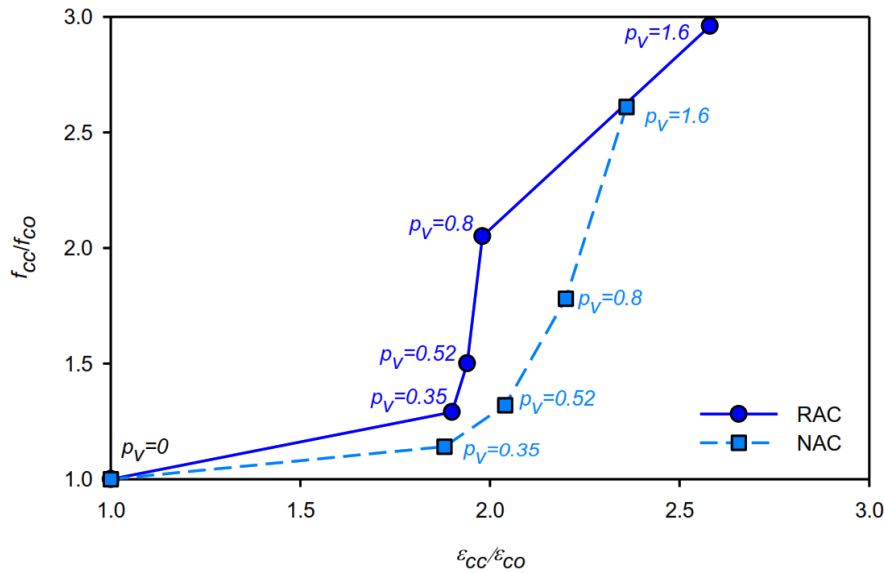


Fig. 8. Relationship between normalised stresses (f_{cc}/f_{co}) and strains ($\epsilon_{cc}/\epsilon_{co}$) as a function of confinement ratios (ρ_v) for RAC and NAC specimens.

3.3 Effect of concrete compressive strength

Fig. 9a shows the confinement ratios for different concrete strengths. The results in **Fig. 9a** indicate an upward trend in confinement ratios as the initial strength decreases. The effective confinement volumetric ratio depends on the initial strength of concrete and its yield strength. As the concrete strength

increases, this ratio decreases, thus reducing the effectiveness of PTMS at improving strength and deformability. This suggests that higher-strength concrete demands more confining material to reach the same effective confinement ratios as low-strength concrete. This observation aligns with findings from a detailed analysis of PTMS on different concrete grades, which revealed that lower initial concrete strengths required higher confinement ratios for effective reinforcement. For instance, M24 grade concrete requires confinement ratios from 0.35 to 1.6 to increase the normalised strength from 1.29 to 2.96. Meanwhile, M21 concrete shows strength increases from 1.44 to 2.92 as confinement ratios rose from 0.40 to 1.83. The lowest strength concrete, M15, benefited the most from high confinement ratios (0.56 to 2.56) to achieve strength enhancements of 1.41 to 2.55 (see **Appendix B**).

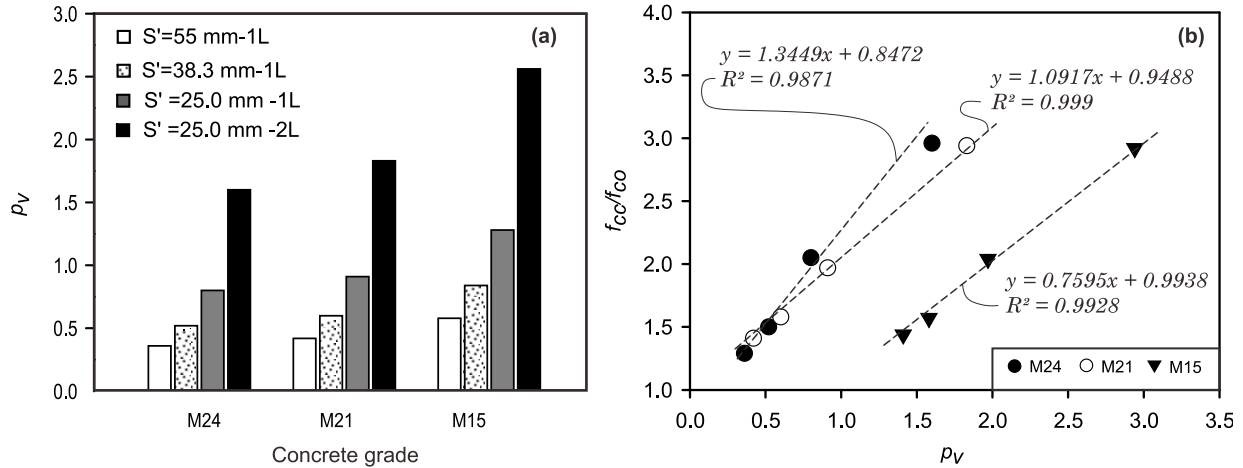


Fig. 9. (a) Confinement ratios vs concrete grade, and (b) normalised concrete strength vs confinement ratios for different concrete strengths.

Fig. 9b compares the normalised concrete strength vs confinement ratios for different concrete strengths. The figure also shows three trend lines for the initial concrete strengths (M24, M21 and M15). The M24 trend line has the sharpest slope ($y = 1.34x + 0.85$), showing a rapid rise in normalised strength as the confinement ratio increases. The high coefficient of determination ($R^2 = 0.987$) suggests a strong data association. The M15 trend line has the shallowest slope ($y = 0.76x + 0.99$), thus indicating slower growth in normalised strength with larger confinement ratios, supported by an $R^2 = 0.993$. The M21 trend line is between the two, with a slope of ($y = 1.09x + 0.95$) and an $R^2 = 0.999$. At a confinement ratio of 0.75, the normalised strength increases by approximately 117% for M24 concrete, 84% for M21 concrete, and 56% for M15 concrete. These percentages highlight the effect of confinement on the normalised strength, with higher initial concrete strengths experiencing more significant benefits from confinement. These results indicate that higher initial concrete strength leads to greater confinement strength with a higher confinement ratio than lower initial strengths. However, more confinement material is needed for higher strength concrete to meet the same effective confinement ratios with low strength concrete. These results suggest that the effectiveness of the PTMS confinement is a function of the concrete strength. The experimental findings presented in previous sections are used in the following section to propose a new constitutive model for RAC cylinders actively confined with PTMS.

4 Analytical study

The utilisation of global stress-strain experimental data for developing stress-strain models for confined concrete has been extensively studied and is recognised as a well-established practice. Mander et al. [50] developed a theoretical model for confined concrete using stress-strain experimental data. Similarly, Kent and Park [51] also proposed a model based on global data from experiments, which has found extensive application in practice. Cusson and Paultre [52] advanced this by creating a model for confined high-strength concrete validated against test results. Saatcioglu and Razvi [53] developed a model that considered the effects of confinement using global data. Sheikh and Uzumeri [54] proposed a model for

tied concrete columns based on global measurements. More recent studies have used global stress-strain data. For example, Zou [55] used finite element analysis (FEM) and digital image correlation (DIC) to assess the behaviour of fibre-reinforced polymer (FRP) confined concrete. Wang et al. [56] developed a new stress-strain model for high-strength concrete confined by lateral ties. This model, validated with global stress-strain data, simplifies the stress-strain relationship while maintaining accuracy.

4.1 Stress-strain results

The stress-strain model is developed based on the M24 RAC confinement test results. Consequently, the detailed discussion of the stress-strain behavior of confined RAC concrete is centered on M24. **Fig. 10** and **Table 5** compare the experimental stress-strain curves of PTMS-confined RAC cylinders. The results demonstrate that higher confinement (ρ_v) improves the concrete's stress and strain behaviour. When ρ_v increased from 0 to 1.6, the peak confined stress and axial strain at failure increased. The compressive strength and deformability increased the most for ρ_v of 0.8 and 1.6. The results in **Fig. 10** also show that the concrete fails gradually after the peak strength, with the steel straps eventually rupturing.

Table 5. Confined stress-strain results

Specimen ID	f_{cc} (MPa)	ϵ_{cc}	ρ_v
Cy-R24-c-1	17.80	0.005	0
Cy-R24-1L55-1	22.95	0.009	0.35
Cy-R24-1L38.30-1	26.71	0.009	0.52
Cy-R24-1L25-1	36.45	0.009	0.80
Cy-R24-2L25-1	52.77	0.012	1.60

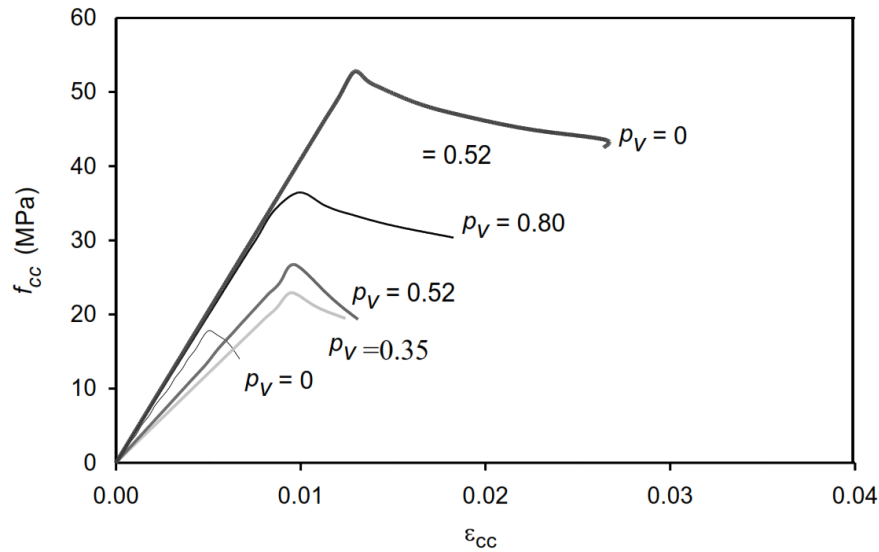


Fig. 10. Stress-strain curves of actively confined RAC cylinders for different confinement ratios.

4.1.1 Peak axial stress

The modified model by Mander et al. [50] is adopted here to describe the stress-strain relationship of concrete confined by steel reinforcement. **Equation 1** can represent the axial stress of steel-confined concrete.

$$\frac{f_{cc}}{f_{co}} = \frac{x \times r}{r - 1 - x^r} \tag{1}$$

where the variables are defined as follows:

$$x = \frac{\epsilon_{cc}}{\epsilon_{co}} \tag{2}$$

$$r = \frac{E_c}{E_c - E_{sec}} \quad (3)$$

$$E_{sec} = \frac{f_{co}}{\varepsilon_{co}} \quad (4)$$

where f_{cc} = confined-concrete compressive strength, x = ratio of longitudinal strain to maximum strain, r = concrete brittleness coefficient, $E_c = 5000\sqrt{f_{co}}$ = modulus of elasticity, and E_{sec} = secant modulus of confined concrete at maximum stress.

Richart et al. [57] proposed a general confinement strength model (**Equation 5**) assuming that the concrete specimens were subjected to hydrostatic pressure:

$$\frac{f_{cc}}{f_{co}} = 1 + k_1 \frac{f_{le}}{f_{co}} \quad (5)$$

where f_{cc} = confined concrete compressive strength, f_{co} = unconfined concrete compressive strength, k_1 = coefficients of confinement effectiveness for strength, and f_{le} = lateral hydrostatic pressure.

Mander et al. [50] provided a more refined prediction model suitable for evaluating the effectiveness of confinement, especially in seismic applications (**Equation 6**):

$$f_{cc} = f_{co} \left(2.254 \sqrt{1 + 7.94 \frac{f_{le}}{f_{co}}} - 2 \frac{f_{le}}{f_{co}} - 1.254 \right) \quad (6)$$

where all variables are as defined before.

The above models can serve as benchmarks for developing further models for active confinement and different concrete, such as RAC.

The confining pressure (f_l), effective confinement pressure (f_{le}) and the effective confinement ratio (ρ_v) can be calculated based on *fib* Model Code 90 [47] according to **Equations (7), (8)** and **(9)**.

$$f_l = 2A_s \times \frac{f_y}{DS'} \quad (7)$$

$$f_{le} = \rho_v \times \frac{f_l}{2} \quad (8)$$

$$\rho_v = \omega_w \times \alpha \left\{ \frac{V_s}{V_c} \frac{f_y}{f_{co}} \right\} \quad (9)$$

$$\omega_w = \frac{A_s 4\pi f_y}{A_g S f_{co}} = \frac{A_s \times 2(b+d) f_y}{bd S f_{co}} \quad (10)$$

where $D = (b^2 + d^2)^{0.5}$, A_s = cross-section area of confinement steel, S' = centre-to-centre spacing of metal straps. Likewise, ω_w = mechanical confinement material ratio as per area, V_s = volume of confining material, V_c = volume of confined concrete, f_y = yield stress of metal, and f_{co} = compressive strength of concrete.

The following section uses the above models (and others available in the literature) to calculate the strength of the PTMS-confined RAC cylinders.

4.1.2 Comparison of strength by existing model's vs test results

Table 6 compares the strength predictions provided by existing models for the PTMS-confined RAC cylinders. The results show that **Frangou's** [14] model is the most reliable among the existing models considered in this study, featuring a mean Prediction/Experimental (Pred./Exp.) ratio of 1.18, mean squared error (MSE) of 0.02, a high coefficient of determination (R^2) of 96%, and a low standard deviation of 0.06. Likewise, **Mander et al.'s** [50] model, with a mean of 1.02 and a standard deviation of 0.08, also

demonstrates high reliability. The **Model Code 90** [47] model also predicts the results well, with a mean of 0.98 and a standard deviation of 0.15. Conversely, **Wu et al.’s** [58] model yields a mean Pred./Exp. of 1.49 and a negative R^2 .

Table 6. Predictions of compressive strength provided by existing models

Models	Mean square error (MSE)	Coefficient of determination (R^2)	Pred./Exp.	Standard deviation (STD)
Frangou [14]	0.02	96%	1.18	0.06
Awang [17]	0.11	76%	1.17	0.13
Lee et al. [32]	1.95	-330%	1.22	0.45
Chin et al. [33]	0.24	47%	0.94	0.14
Moghaddam et al.[42]	0.63	-3.8%	1.11	0.26
Model Code 90 [47]	0.11	77%	0.98	0.15
Mander et al. [50]	0.04	90%	1.02	0.08
Richart et al. [57]	0.77	-69%	1.08	0.31
Wu et al. [58]	1.42	-215%	1.49	0.27
Saatcioglu and Razvi [59]	0.72	-58%	1.14	0.27
Shah et al. [60]	0.18	60%	1.16	0.11
Lim and Ozbakkaloglu [61]	0.64	-42%	1.12	0.26

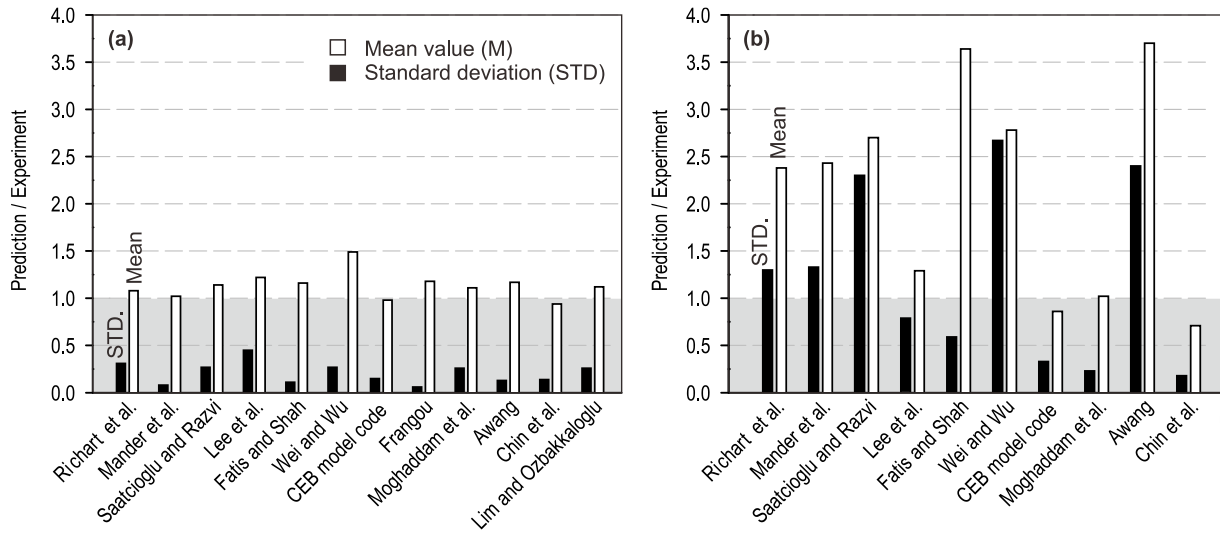


Fig. 11. Comparison of (a) strength and (b) strain predictions by existing confinement models found in the literature.

Fig. 11a and **Fig.11b** compare, respectively, the compressive strength and axial strain predictions provided by existing confinement models for the PTMS-confined RAC cylinders. The results indicate that some models reasonably predict the results of the PTMS-confined RAC cylinders tested in this study, although most models tend to overpredict the results. These discrepancies were expected since the existing models were developed for NAC cylinders. The different mechanical behaviour between NAC and RAC suggests the need for developing a new confinement model for PTMS-confined RAC cylinders. Such a new model is also necessary to produce design tools (e.g. [62-65]), which in turn promote the broader adoption of PTMS in practice. As a result, sections 4.1.3 and 4.1.4 propose new empirical models based on statistical polynomial regressions from the experimental results presented in previous sections. A validation of the proposed models is also provided.

4.1.3 Ultimate axial strength prediction model

Fig. 5a illustrates that the strength gained from PTMS confinement does not exhibit a fully linear relationship with increasing confinement ratios. Thus, **Equation 11** is introduced here to estimate the strength of RAC cylinders confined with PTMS. This empirical equation adopts statistical regression

techniques to correlate the confinement ratios and the confined strength of RAC cylinders. To achieve this, Python coding and Excel regression analyses were adopted. This statistical analysis sufficiently captured the PTMS-confined RAC's complex linear and non-linear relationship.

$$\frac{f_{cc,RAC}}{f_{co,RAC}} = 0.972 + 1.23 \times \rho_v^{1.015} \tag{11}$$

Fig. 12 shows that the proposed model predicts the normalised strength (f_{cc}/f_{co}) as a function of confinement ratio (ρ_v) well, as the prediction closely aligns with the data points from various other predictive models and test results. Indeed, **Equation 11** yields a high R^2 value of 98.6%, thus indicating that the model accurately captures the variance in the test results. Similarly, the model estimates well the confined strength of the tested cylinders, achieving a Pred./Exp mean value of 1.0 with a standard deviation of 0.05. The power on the confinement ratio (ρ_v) considers that the confinement ratio and confined strength do not have a perfect linear relationship. The model indicates that each unit increase in ρ_v enhances the ratio f_{cc}/f_{co} by approximately 1.23, with an intercept of 0.972. Whilst some outliers exist in the data (particularly at high confinement ratios), they are relatively independent of the model's overall reliability. Consequently, the newly suggested model is considered appropriate for predicting the strength of PTMS-confined concrete cylinders.

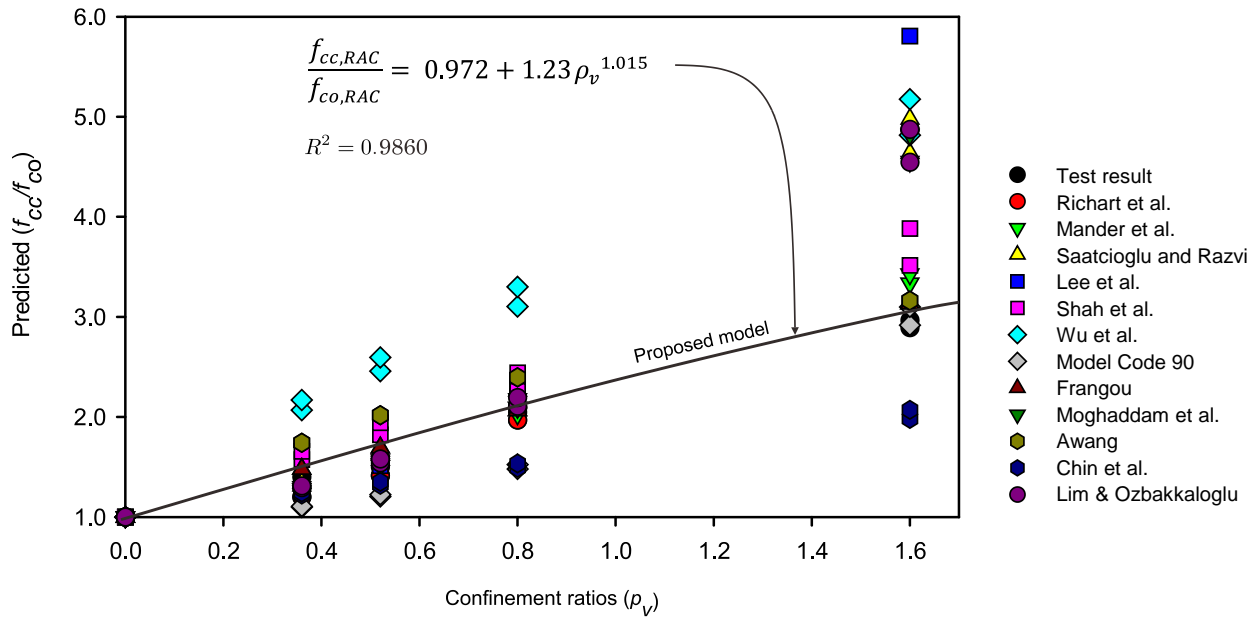


Fig. 12. Prediction of normalised PTMS-confined strength given by proposed model (Eq. 11) and other confinement models in the literature.

4.2 Peak axial strain

4.2.1 Comparison of existing model vs test results

Table 7 compares the strain predictions provided by existing models for PTMS-confined RAC cylinders. The results show that **Moghaddam et al.’s** [42] model predicts the experimental results well (Pred./Exp. = 1.02, standard deviation = 0.23). The other models have negative R^2 values, indicating a poor fit to the experimental results. These findings suggest the necessity for a new model to predict the peak strain of PTMS-confined RAC cylinders.

Table 7. Prediction of axial strain provided by existing models

Models	Mean square error (MSE)	Coefficient of determination (R^2)	Pred./Exp.	Standard deviation (STD)
Awang [17]	66.4	-295	3.70	2.40
Lee et al. [32]	3.55	-14.84	1.29	0.79
Chin et al. [33]	0.36	-0.62	0.71	0.18
Moghaddam et al.[42]	0.19	0.26	1.02	0.23
Model Code 90 [47]	0.51	-1.28	0.86	0.33
Mander et al. [50]	17.66	-68.24	2.43	1.33
Richart et al. [57]	17.66	-68.24	2.38	1.30
Wu et al. [58]	55.09	-244.00	2.78	2.67
Saatcioglu and Razvi [59]	43.56	-169.78	2.7	2.30
Shah et al. [60]	0.09	0.57	3.64	0.59

4.2.2 Peak axial strain prediction model

The variability in strain results indicates that a polynomial regression with two independent variables (normalised strain and confinement ratios) is suitable for proposing an empirical model for PTMS-confined RAC cylinders. The statistical polynomial regression correlated the ratios of $\epsilon_{cc}/\epsilon_{co}$ to f_{cc}/f_{co} and ρ_v (see **Fig. 13**), thus leading to **Equation 12**. As such, **Equation 12** calculates the peak strain (corresponding to ultimate stress) of PTMS-confined RAC cylinders:

$$\frac{\epsilon_{cc,RAC}}{\epsilon_{co,RAC}} = 2.85 - 1.95 \frac{f_{cc}}{f_{co}} + 4.03\rho_v + 0.13 \left(\frac{f_{cc}}{f_{co}} \right)^2 - 0.89\rho_v^2 \tag{12}$$

Fig. 13 and **Equation 12** also show a coefficient of determinacy $R^2= 96.99\%$ and an MSE= 0.0067, indicating that the suggested model can reliably predict the strains in PTMS-confined RAC cylinders. Moreover, **Equation 12** leads to a mean Pred./Exp ratio of 1.0 and a standard deviation of 0.05.

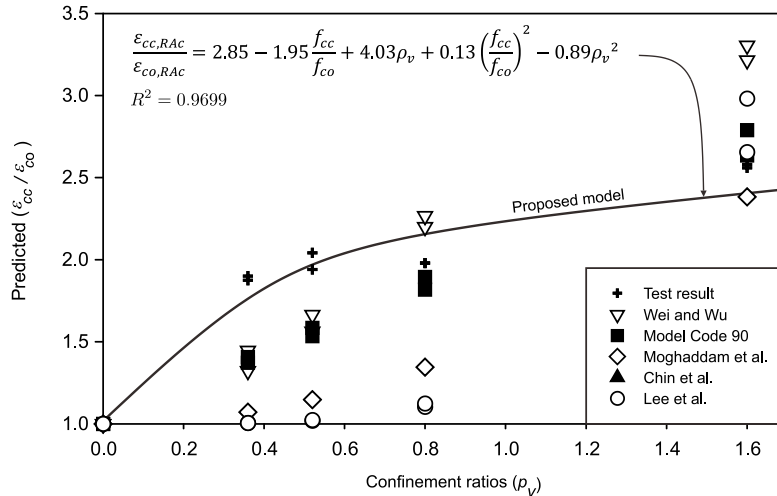


Fig.13. Prediction of normalised PTMS-confined strain given by proposed model (Eq. 12) and other confinement models in the literature.

4.3 Comparison with experimental results

Table 8 compares the predictions by the suggested model (**Equations 11 and 12**) and the test results obtained from the PTMS-confined RAC cylinders, including the Pred./Exp. ratio. Likewise, **Fig. 14** compares the stress-strain relationships given by the new suggested model vs the experimental curves. The results indicate that **Equations 11 and 12** predict the strength and strain values of PTMS-confined RAC cylinders well. **Equation 11** leads to low error rates and a high R^2 value of 98.6%. Likewise, **Equation 12** has an R^2 of 96.99% and adequately predicts the strain of PTMS-confined RAC cylinders (see **Fig. 14**).

Table 8. Stress-strain predictions given by proposed model vs experimental results

Specimen ID	ρ_v	Experimental values		Predicted values		Pred./Exp.	
		f_{cc}/f_{cc}	$\epsilon_{cc}/\epsilon_{co}$	f_{cc}/f_{co}	$\epsilon_{cc}/\epsilon_{co}$	Stress	Strain
Cy-R24-c-1	0.00	1.00	1.00	1.00	1.00	0.97	1.03
Cy-R24-c-2	0.00	1.00	1.00	1.00	1.00	0.97	1.03
Cy-R24-1L55-1	0.35	1.29	1.90	1.44	1.83	1.09	0.99
Cy-R24-1L55-2	0.35	1.40	1.88	1.44	1.66	1.01	0.91
Cy-R24-1L38.30-1	0.52	1.50	1.94	1.65	2.01	1.07	1.07
Cy-R24-1L38.30-2	0.52	1.59	2.04	1.65	1.88	1.01	0.95
Cy-R24-1L25-1	0.80	2.05	1.98	2.01	2.00	0.95	1.04
Cy-R24-1L25-2	0.80	2.10	1.98	2.01	1.92	0.93	1.00
Cy-R24-2L25-1	1.60	2.96	2.58	3.03	2.31	1.00	0.98
Cy-R24-2L25-2	1.60	2.89	2.56	3.03	2.40	1.02	1.00
Standard Deviation (STD)						0.05	0.05
Mean Values						1.00	1.00

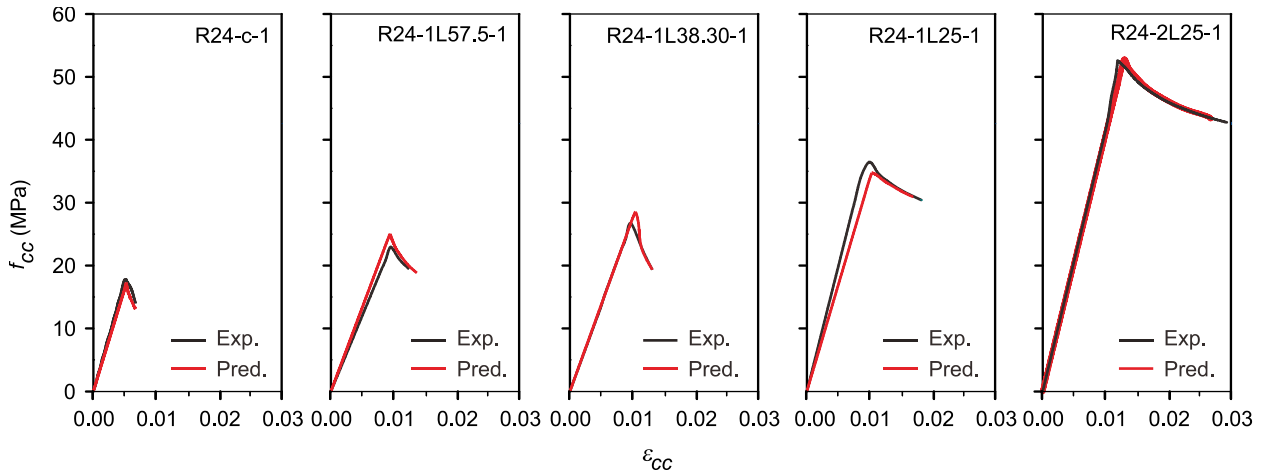


Fig. 14. Comparison of stress-strain relationship given by proposed model vs experimental curves.

It should be pointed out that the suggested model is only applicable for high RCA contents, such as the ones in this study, where all of the coarse aggregate contains RCA. To date, there is no additional literature on PTMS-confined RAC cylinders with large volumes of RCA. Thus, more studies are required to confirm the model's validity using other experimental datasets and to extend the model to incorporate different amounts of RCA. Moreover, the experiments performed here did not cover the descending part of the stress-strain behaviour, and therefore this is a matter of future research. Further research should also investigate other variables such as shape (square, rectangular) to assess the confinement effectiveness, and the height of specimen to assess the effects of slenderness on the response of RAC elements.

5 Conclusions and recommendations

This study proposes a new constitutive model for recycled aggregate concrete cylinders actively confined with PTMS. RAC cylinders ($\phi 150 \times 300$ mm) with different confinement ratios ($\rho_v = 0, 0.35, 0.52, 0.80$ or 1.6) were subjected to axial compression until failure to determine their maximum strength and axial strains. The RAC was produced using RCA as coarse aggregate, considering three compressive strengths: 15 MPa (M15), 21 MPa (M21) and 24 MPa (M24). Based on the test results and on regression analyses, a new stress-strain constitutive model is proposed to assess the effectiveness of the PTMS confinement on RAC cylinders. Key conclusions from this research are:

- The active confinement provided by the PTMS improved the strength and deformability of RAC

cylinders. For confinement ratios (ρ_v) of 0.35, 0.52, 0.80, and 1.6, the enhancements were 29%, 50%, 105%, and 196%, respectively. Likewise, the PTMS confinement increased the axial strains by 90% to 158%, corresponding to the confinement ratios of 0.35 and 1.6, respectively.

- The test results show that higher initial concrete strengths resulted in a more pronounced increase in confined strength with increasing confinement ratios due to the higher effectiveness of the PTMS technique. At a confinement ratio of 0.75, the strength increased by approximately 117% for M24, 84% for M21, and 56% for M15, demonstrating that higher initial concrete strengths benefit more from confinement.
- Based on the experimental results, a novel constitutive model for PTMS-confined RAC cylinders was presented. The suggested model estimated the strength and strain of the tested cylinders based on the confinement ratio. The model's prediction-to-experiment ratio (Pred./Exp.) was 1.0, with a standard deviation 0.05.

It is important to note that the suggested model is only applicable to high RCA contents like those used in this study (with coarse aggregate made entirely of RCA). Research on PTMS-confined RAC cylinders containing high volumes of RCA is currently lacking in the literature. Thus, additional research is needed to confirm the model's accuracy with different experimental datasets and to expand the model's applicability to other RCA proportions. Further research should also investigate other variables such as shape (square, rectangular) and height to assess the effects of confinement effectiveness and slenderness on the response of RAC elements.

Acknowledgements

The project was supported by the Walailak University International Mobility Fund for Research collaboration program (Contract no. WU-CIA-05107/2024).

Funding Statement

Walailak University Graduate Scholarships have supported this work.

CRedit authorship contribution statement

Ram Prasad Neupane: Investigation, Formal analysis, Writing—original draft. **Thanongsak Imjai:** Conceptualisation, Funding acquisition, Supervision, Investigation, Formal analysis, Writing—original draft. **Reyes Garcia:** Supervision, Investigation, Writing—review and editing. **U. Johnson Alengaram:** Supervision, Investigation.

Conflicts of Interest

The authors declare no conflicts of interest to report regarding the present study.

References

- [1] Thomas J, Thaickavil NN, Wilson PM. Strength and durability of concrete containing recycled concrete aggregates. *J Build Eng.* 2018; 19: 349-65. doi:10.1016/j.jobe.2018.05.007.
- [2] Chakradhara Rao M. Properties of recycled aggregate and recycled aggregate concrete: effect of parent concrete. *Asian J Civ Eng.* 2018; 19(1): 103-10. doi:10.1007/s42107-018-0011-x.
- [3] Zhou C, Chen Z. Mechanical properties of recycled concrete made with different types of coarse aggregate. *Constr Build Mater.* 2017; 134: 497-506. doi:10.1016/j.conbuildmat.2016.12.163.
- [4] Imjai T., Setkit, M, Figueiredo, FP, Garcia R, Sae-Long, W, Limkatanyu S. Experimental and numerical investigation on low-strength RC beams strengthened with side or bottom near surface mounted FRP rods. *Struct Infrastruct Eng.* 2023; 19(11): 1600-1615. doi.org/10.1080/15732479.2022.2045613
- [5] Arezoumandi M, Drury J, Volz JS, Khayat KH. Effect of recycled concrete aggregate replacement level on shear strength of reinforced concrete beams. *ACI Mater J.* 2015; 112(4): 559-68. doi:10.14359/51687766.
- [6] Rahal KN, Alrefaei YT. Shear strength of recycled aggregate concrete beams containing stirrups. *Constr Build Mater.* 2018; 191: 866-76. doi:10.1016/j.conbuildmat.2018.10.023.

- [7] Wang B, Yan L, Fu Q, Kasal B. A comprehensive review of recycled aggregate and recycled aggregate concrete. *Resour Conserv Recycl.* 2021; 171: 105565. doi:10.1016/j.resconrec.2021.105565.
- [8] Mohanta NR, Murmu M. Alternative coarse aggregate for sustainable and eco-friendly concrete - A review. *J Build Eng.* 2022; 59: 105079. doi:10.1016/j.jobee.2022.105079.
- [9] Verian KP, Ashraf W, Cao Y. Properties of recycled concrete aggregate and their influence in new concrete production. *Resour Conserv Recycl.* 2018; 133: 30-49. doi:10.1016/j.resconrec.2018.02.0050.
- [10] González-Taboada I, González-Fontboa B, Martínez-Abella F, Carro-López D. Study of recycled concrete aggregate quality and its relationship with recycled concrete compressive strength using database analysis. *Mater Struct.* 2016; 66: 323. doi:10.3989/mc.2016.06415.
- [11] Neupane RP, Imjai T, Makul N, Garcia R, Kim B, Chaudhary S. Use of recycled aggregate concrete in structural members: A review focused on Southeast Asia. *J Asian Archit Build Eng.* 2023; 00(00): 1-24. doi:10.1080/13467581.2023.2270029.
- [12] Alhawat M, Ashour A. Bond strength between corroded steel and recycled aggregate concrete incorporating nano-silica. *Constr Build Mater.* 2020; 237: 117441. doi:10.1016/j.conbuildmat.2019.117441.
- [13] Leelatanon S, Imjai T, Setkit M, Garcia R, Kim, B. Punching shear capacity of recycled aggregate concrete slabs. *Buildings.* 2022; 12(10): 1584. doi: 10.3390/buildings12101584.
- [14] Frangou M. Strengthening of concrete by lateral confinement. Sheffield: University of Sheffield, Department of Civil and Structural Engineering; 1996.
- [15] Imjai T, Setkit M, Garcia R, Figueiredo FP. Strengthening of damaged low-strength concrete beams using PTMS or NSM techniques. *Case Stud Constr Mater.* 2020; 13; e00403. doi.org/10.1016/j.cscm.2020.e00403
- [16] Ma CK, Garcia R, Yung SCS, Awang AZ, Omar W, Pilakoutas K. Strengthening of pre-damaged concrete cylinders using post-tensioned steel straps. *Proc Inst Civ Eng Struct Build.* 2019; 172(10): 703-11. doi:10.1680/jstbu.18.00031.
- [17] Awang AZ. Stress-strain behaviour of high-strength concrete with lateral pre-tensioning confinement. Johor Bahru: Universiti Teknologi Malaysia; 2013.
- [18] Lee HP, Awang AZ, Omar W. Steel strap confined high strength concrete under uniaxial cyclic compression. *Constr Build Mater.* 2014; 72: 48-55. doi:10.1016/j.conbuildmat.2014.08.007.
- [19] Samadi M, Moghaddam H, Pilakoutas K. Seismic retrofit of RC columns with inadequate lap-splice length by external post-tensioned high-strength strips. In: 15th World Conference on Earthquake Engineering; 2012; Paper no. 1995.
- [20] Ma CK, Awang AZ, Omar W, Liang M, Jaw SW, Azimi M. Flexural capacity enhancement of rectangular high-strength concrete columns confined with post-tensioned steel straps: experimental investigation and analytical modelling. *Struct Concr.* 2016; 17(4): 668-76. doi:10.1002/suco.201500123.
- [21] Garcia R, Hajirasouliha I, Guadagnini M, Helal Y, Jemaa Y, Pilakoutas K, Saiidi M. Full-scale shaking table tests on a substandard RC building repaired and strengthened with post-tensioned metal straps. *J Earthq Eng.* 2014; 18(2): 187-213. <https://doi.org/10.1080/13632469.2013.847874>.
- [22] Helal, Y, Garcia R, Imjai T, Aosai P, Guadagnini M, Pilakoutas, K. Seismic behaviour of exterior RC beam-column joints repaired and strengthened using post-tensioned metal straps. *Bull Earthq Eng.* 2024; 22(6): 3261-3286. <https://doi.org/10.1007/s10518-024-01904-1>.
- [23] Setkit M, Imjai T, Chaisakulkiet U, Garcia R, Danyem K, Sanupong K, Chamnankit W. Torsional strengthening of low-strength RC beams with post-tensioned metal straps: An experimental investigation. *Walailak J Sci & Tech.* 2020; 17(12): 1399-1411. doi:10.48048/wjst.2020.11908.
- [24] Imjai T, Chaisakulkiet U, Garcia R, Pilakoutas K. Strengthening of RC members using post-tensioned metal straps: State of the research. *Lowl Technol Int.* 2018; 20(2): 187-96.
- [25] Rodsin K, Hussain Q, Suparp S, Nawaz A. Compressive behaviour of extremely low strength concrete confined with low-cost glass FRP composites. *Case Stud Constr Mater.* 2020; 13. doi:10.1016/j.cscm.2020.e00452.
- [26] Imjai T, Setkit M, Garcia R, Sukontasukkul P, Limkatanyu S. Seismic strengthening of low strength concrete columns using high ductile metal strap confinement: A case study of a kindergarten school in northern Thailand. *Walailak J Sci & Tech* 2020; 17(12): 1335-1347. doi:10.48048/wjst.2020.10738
- [27] Raffoul S, Escolano-Margarit D, Garcia R, Guadagnini M, Pilakoutas K. Constitutive model for rubberised concrete passively confined with FRP laminates. *J Compo. Constr.* 2019; 23(6): 4019044. [https://doi.org/10.1061/\(ASCE\)CC.1943-5614.0000972](https://doi.org/10.1061/(ASCE)CC.1943-5614.0000972).
- [28] Ma H, Qiang J, Xi J, Zhao Y. Cyclic loading tests and horizontal bearing capacity of recycled concrete filled circular steel tube and profile steel composite columns. *J Constr Steel Res.* 2022; 199: 107572. doi:10.1016/j.jcsr.2022.107572.
- [29] Han Q, Yuan WY, Ozbakkaloglu T, Bai YL, Du XL. Compressive behaviour for recycled aggregate concrete

- confined with recycled polyethylene naphthalate/terephthalate composites. *Constr Build Mater.* 2020; 261: 120498. doi:10.1016/j.conbuildmat.2020.120498.
- [30] Frangou M, Pilakoutas K, Dritsos S. Structural repair/strengthening of RC columns. *Constr Build Mater.* 1995; 9(5): 259–266. doi:10.1016/0950-0618(95)00013-6.
- [31] Moghaddam H, Samadi M, Pilakoutas K. Compressive behaviour of concrete actively confined by metal strips, part B: Analysis. *Mater Struct Constr.* 2010; 43(10): 1383–1396. doi:10.1617/s11527-010-9589-5.
- [32] Lee HP, Awang AZ, Omar W. Strength and ductility of high-strength concrete cylinders externally confined with steel strapping tensioning technique (SSTT). *J Teknol.* 2014; 68(1): 11.
- [33] Chin C, Ma C, Awang AZ, Omar W, Kueh ABH. Stress-strain evaluation of steel-strapped high-strength concrete with modified self-regulating end clips. *Struct Concr.* 2018; 19(4): 1036–1048. doi:10.1002/suco.201700134.
- [34] American Concrete Institute (ACI). ACI 211.1-91: Standard Practice for Selecting Proportions for Normal, Heavyweight, and Mass Concrete. American Concrete Institute, 1991.
- [35] Grübl P, Rübl M. German Committee for Reinforced Concrete (DAFFSTB)-Code: Concrete with Recycled Aggregates. In *Sustainable Construction: Use of Recycled Concrete Aggregate: Proceedings of the International Symposium organised by the Concrete Technology Unit, University of Dundee and held at the Department of Trade and Industry Conference Centre, London, UK on 11–12 November 1998*, (pp. 409-418). Thomas Telford Publishing.
- [36] NTC 2008. Technical Standards for Construction, Norme Tecniche per le Costruzioni, Italy, 2008.
- [37] JIS A 5022, Recycled aggregate concrete-Class M. Japanese Standards Association, 2018.
- [38] BS EN 206-1: Specification for Constituent Materials and Concrete. British Standards Institution, London; 2006.
- [39] BS EN 12390-3: Testing hardened concrete – Part 3: Compressive strength of test specimens, British Standards Institution, London; 2002.
- [40] BS EN 12390-6: Testing hardened concrete – Part 6: Splitting tensile strength of test specimens, British Standards Institution, London; 2010.
- [41] BS EN 12390-5: Testing hardened concrete – Part 5: Making and curing specimens for strength tests. British Standards Institution, London; 2009.
- [42] Moghaddam H, Samadi M, Pilakoutas K, Mohebbi S. Axial compressive behavior of concrete actively confined by metal strips; Part A: Experimental study. *Mater Struct Constr.* 2010; 43(10): 1369-1381. doi: 10.1617/s11527-010-9588-6.
- [43] Lee HP, Awang AZ, Omar W. Steel strap confined high strength concrete under uniaxial cyclic compression. *Constr Build Mater.* 2014; 72: 48–55. doi:10.1016/j.conbuildmat.2014.08.007.
- [44] Yang Y, Xue Y, Yu Y, Li Y. Research on axial behaviour of concrete columns retrofitted with pre-stressed steel strips. *Mag Concr Res.* 2020; 72(21): 1089–1101. doi:10.1680/jmacr.18.00107.
- [45] Ma CK, Awang AZ, Garcia R, Omar W, Pilakoutas K. Behaviour of over-reinforced high-strength concrete beams confined with post-tensioned steel straps – an experimental investigation. *Struct Concr.* 2016; 17(5): 768–777. doi: 10.1002/suco.201500062.
- [46] European Committee for Standardization (CEN). Eurocode 8: Design of Structures for Earthquake Resistance – Part 3: Assessment and Retrofitting of Buildings (EN 1998-3:2005).
- [47] Comité Euro-International du Béton. (1993). CEB-FIP Model Code 1990: Design code (Vol. 1). Thomas Telford.
- [48] Helal Y, Garcia R, Pilakoutas K, Guadagnini M, Hajirasouliha I. Bond of substandard laps in reinforced concrete beams retrofitted with post-tensioned metal straps. *ACI Struct J.* 2016; 113(6). <https://doi.org/10.14359/51689021>.
- [49] Helal Y, Garcia R, Pilakoutas K, Guadagnini M, Hajirasouliha I. Strengthening of short splices in RC beams using Post-Tensioned Metal Straps. *Mater Struct Constr.* 2016; 49(1-2): 133–147. doi:10.1617/s11527-014-0481-6.
- [50] Mander JB, Priestley MJN, Park R. Theoretical stress-strain model for confined concrete. *J Struct Eng.* 1988; 114(8): 1804–1826. doi:10.1061/(ASCE)0733-9445(1988)114:8(1804).
- [51] Kent DC, Park R. Flexural members with confined concrete. *J Struct Div.* 1971; 97(7): 1969–1990. doi:10.1061/JSDEAG.0002957.
- [52] Cusson D, Paultre P. Stress-strain model for confined high-strength concrete. *J Struct Eng.* 1995; 121(3): 468–477. doi:10.1061/(ASCE)0733-9445(1995)121:3(468).
- [53] Saatcioglu M, Razvi SR. Strength and ductility of confined concrete. *J Struct Eng.* 1992; 118(6): 1590–1607. doi:10.1061/(ASCE)0733-9445(1992)118:6(1590).
- [54] Sheikh SA, Uzumeri SM. Strength and ductility of tied concrete columns. *J Struct Div.* 1980; 106(5): 1079–1102. doi:10.1061/JSDEAG.0005416.
- [55] Zou Y. Evaluation of the strain response of FRP partially confined concrete using FEM and DIC testing. *Int J*

- Struct Integr. 2024. doi:10.1108/IJSI-11-2023-0112.
- [56] Wang L, Huang X, Xu F. Stress-Strain Model of High-Strength Concrete Confined by Lateral Ties under Axial Compression. *Buildings*. 2023; 13(4): 870. doi:10.3390/buildings13040870.
- [57] Richart FE, Brandtæg A, Brown RL. Failure of plain and spirally reinforced concrete in compression. *Univ of Illinois Eng Exp Station Bull*. 1929; (190).
- [58] Wu YF, Yun Y, Wei Y, Zhou Y. Effect of pre-damage on the stress-strain relationship of confined concrete under monotonic loading. *J. Struct. Eng.* 2014; 140(12): 1-18. doi:10.1061/(ASCE)ST.1943-541X.0001015.
- [59] Murat S, R. S. R. Strength and Ductility of Confined Concrete. *J Struct Eng.* 1992; 118(6): 1590–1607. doi:10.1061/(ASCE)0733-9445(1992)118:6(1590).
- [60] Shah SP, Apostolos F, Anderson R. Cyclic loading of spirally reinforced concrete. *J Struct Eng.* 1983; 109(7): 1695–1710. doi:10.1061/(ASCE)0733-9445(1983)109:7(1695).
- [61] Lim JC, Ozbakkaloglu T. Stress-strain model for normal- and lightweight concrete under uniaxial and triaxial compression. *Constr Build Mater.* 2014; 71: 492–509. doi:10.1016/j.conbuildmat.2014.08.050.
- [62] Khun MC, et al. Design of steel-strapped, high-strength concrete columns subject to unequal end moments. *Proc Inst Civ Eng Struct Build.* 2018; 171(4): 273–282. doi:10.1680/jstbu.15.00072.
- [63] Neupane RP, Imjai T, Garcia R, Chua YS, Chaudhary S. Performance of eccentrically loaded low-strength RC columns confined with post-tensioned metal straps: an experimental and numerical investigation. *Struct Concr* 2024. doi.org/10.1002/suco.202301026.
- [64] Chau-Khun M, Awang AZ, Omar W, Pilakoutas K, Tahir MM, Garcia R. Elastic design of slender high-strength RC circular columns confined with external tensioned steel straps. *Adv Struct Eng.* 2015; 18(9): 1487–1499. doi:10.1260/1369-4332.18.9.1487.
- [65] Chau-Khun M, Awang AZ, Garcia R, Omar W, Pilakoutas K, Azimi M. Nominal Curvature Design of Circular HSC Columns Confined with Post-tensioned Steel Straps. *Structures* 2016; 7: 25–32. <https://doi.org/10.1016/j.istruc.2016.04.002>.

Appendix A: Details of tested cylinders

Specimen ID	Concrete type	d mm	h mm	S' (mm)	n	f_{le} (MPa)	p_v	Remarks
Cy-R24-c-1	RAC- 24	151.58	304.82	0	0	0	0	Control
Cy-R24-c-2	RAC- 24	151.58	304.82	0	0	0	0	Control
Cy-R24-1L55-1	RAC- 24	151.58	304.82	55.00	1.00	0.73	0.35	
Cy-R24-1L55-2	RAC- 24	151.58	304.82	55.00	1.00	0.73	0.35	
Cy-R24-1L38.30-1	RAC- 24	151.58	304.82	38.30	1.00	1.64	0.52	
Cy-R24-1L38.30-2	RAC- 24	151.58	304.82	38.30	1.00	1.64	0.52	
Cy-R24-1L25-1	RAC- 24	151.58	304.82	25.00	1.00	3.84	0.8	
Cy-R24-1L25-2	RAC- 24	151.58	304.82	25.00	1.00	3.84	0.8	
Cy-R24-2L25-1	RAC- 24	151.58	304.82	25.00	2.00	15.36	1.6	
Cy-R24-2L25-2	RAC- 24	151.58	304.82	25.00	2.00	15.36	1.6	
Cy-N24-c-1	NAC -24	151.58	304.82	0	0	0	0	Control
Cy-N24-L55-1	NAC -24	151.58	304.82	55.00	1.00	0.73	0.35	
Cy -N24-1L38.30-1	NAC -24	151.58	304.82	38.30	1.00	1.64	0.52	
Cy-N24-1L25-1	NAC -24	151.58	304.82	25.00	1.00	3.84	0.8	
Cy-N24-2L25-1	NAC -24	151.58	304.82	25.00	2.00	15.36	1.6	
Cy-R21-c-1	RAC- 21	151.58	304.82	0	0	0	0	Control
Cy-R21-1L-55-1	RAC- 21	151.58	304.82	55.00	1.00	0.83	0.40	
Cy-R21-1L-38.3-1	RAC- 21	151.58	304.82	38.30	1.00	1.87	0.60	
Cy-R21-1L-25-1	RAC- 21	151.58	304.82	25.00	1.00	4.39	0.91	
Cy-R21-2L-25-1	RAC- 21	151.58	304.82	25.00	2.00	17.55	1.83	
Cy-N21-c-1	RAC- 21	151.58	304.82	0	0	0	0	Control
Cy-N21-1L-55-1	RAC- 21	151.58	304.82	55.00	1.00	0.83	0.40	
Cy-N21-1L-38.3-1	RAC- 21	151.58	304.82	38.30	1.00	1.87	0.60	
Cy-N21-1L-25-1	RAC- 21	151.58	304.82	25.00	1.00	4.39	0.91	
Cy-N21-2L-25-1	RAC- 21	151.58	304.82	25.00	2.00	17.55	1.83	
Cy-R15-c-1	RAC- 15	151.58	304.82	0	0	0	0	Control
Cy-R15-1L-55-1	RAC- 15	151.58	304.82	55.00	1.00	1.16	0.56	
Cy-R15-1L-38.3-1	RAC- 15	151.58	304.82	38.30	1.00	2.62	0.84	
Cy-R15-1L-25-1	RAC- 15	151.58	304.82	25.00	1.00	6.14	1.28	
Cy-R15-2L-25-1	RAC- 15	151.58	304.82	25.00	2.00	24.58	2.56	
Cy-N15-c-1	NAC- 15	151.58	304.82	0	0	0	0	Controlled
Cy-N15-1L-55-1	NAC- 15	151.58	304.82	55.00	1.00	1.16	0.56	
Cy-N15-1L-38.3-1	NAC- 15	151.58	304.82	38.30	1.00	2.62	0.84	
Cy-N15-1L-25-1	NAC- 15	151.58	304.82	25.00	1.00	6.14	1.28	
Cy-N15-2L-25-1	NAC- 15	151.58	304.82	25.00	2.00	24.58	2.56	

Note: D = diameter of cylinder specimen, h = height of specimen, S' = spacing of PTMS, n = number of metal strap layers, f_{le} = effective confinement pressure, p_v = effective volumetric confinement ratio.

Appendix B: Summary of the experimental result of tested specimens

Specimen ID	P (kN)	δ (mm)	f_{cc} (MPa)	f_{cc}/f_{co}	ϵ_{cc}	$\epsilon_{cc}/\epsilon_{co}$	f_{ie} (MPa)	ρ_v	Remarks
Cy-R24-c-1	321.29	1.53	17.80	1.00	0.005	1.00	0	0	Control
Cy-R24-c-2	293.67	1.45	16.27	1.00	0.0048	1.00	0	0	
Cy-R24-1L55-1	414.16	2.90	22.95	1.29	0.0095	1.90	0.73	0.35	
Cy-R24-1L57-2	410.70	2.75	22.76	1.40	0.009	1.88	0.73	0.35	
Cy-R24-1L38.30-1	481.97	2.97	26.71	1.50	0.0097	1.94	1.64	0.52	
Cy-R24-1L38.30-2	466.51	2.99	25.85	1.59	0.0098	2.04	1.64	0.52	
Cy-R24-1L25-1	657.71	3.01	36.45	2.05	0.0099	1.98	3.84	0.8	
Cy-R24-1L25-2	617.63	2.89	34.23	2.10	0.0095	1.98	3.84	0.8	
Cy-R24-2L25-1	952.21	3.21	52.77	2.96	0.0122	2.44	15.36	1.6	
Cy-R24-2L25-2	848.73	3.79	47.03	2.89	0.0118	2.46	15.36	1.6	
Cy-N24-c-1	399.62	1.15	22.145	1.00	0.004	1.00	0	0	Control
Cy-N24-L55-1	456.21	2.16	25.281	1.14	0.008	1.88	0.73	0.35	
Cy-N24-1L38.30-1	527.11	2.35	29.210	1.32	0.007	2.04	1.64	0.52	
Cy-N24-1L25-1	711.57	2.53	39.431	1.78	0.009	2.20	3.84	0.8	
Cy-N24-2L25-1	1041.96	2.71	57.740	2.61	0.008	2.36	15.36	1.6	
Cy-R21-c-1	283.62	1.58	15.72	1.00	0.010	1.00	0	0	Control
Cy-R21-1L-55-1	399.68	2.22	22.15	1.41	0.01	1.41	0.83	0.40	
Cy-R21-1L-38.3-1	447.87	2.00	24.82	1.58	0.01	1.27	1.87	0.60	
Cy-R21-1L-25-1	558.93	2.99	28.09	1.97	0.02	1.89	4.39	0.91	
Cy-R21-2L-25-1	833.24	3.88	40.14	2.94	0.019	2.46	17.55	1.83	
Cy-N21-c-1	319.75	2.03	17.72	1.00	0.013	1.00	0	0	Control
Cy-N21-1L-55-1	414.32	4.00	22.96	1.30	0.026	1.97	0.83	0.40	
Cy-N21-1L-38.3-1	484.78	1.80	26.86	1.52	0.012	0.89	1.87	0.60	
Cy-N21-1L-25-1	548.61	3.75	30.40	1.72	0.025	1.85	4.39	0.91	
Cy-N21-2L-25-1	851.26	2.78	47.17	2.66	0.018	1.37	17.55	1.83	
Cy-R15-c-1	242.68	0.64	13.45	1.00	0.004	1	0	0	Control
Cy-R15-1L-55-1	348.58	1.00	19.32	1.44	0.01	1.56	1.16	0.56	
Cy-R15-1L-38.3-1	382.02	1.56	21.17	1.57	0.01	2.44	2.62	0.84	
Cy-R15-1L-25-1	493.92	2.95	27.37	2.04	0.02	4.61	6.14	1.28	
Cy-R15-2L-25-1	709.17	3.36	39.30	2.92	0.02	5.25	24.58	2.56	
Cy-N15-c-1	280.03	1.69	15.52	1.00	0.011	1.00	0	0	Control
Cy-N15-1L-55-1	350.29	3.94	19.41	1.25	0.026	2.33	1.16	0.56	
Cy-N15-1L-38.3-1	416.85	4.14	23.10	1.49	0.027	2.45	2.62	0.84	
Cy-N15-1L-25-1	514.68	4.66	28.52	1.84	0.031	2.76	6.14	1.28	
Cy-N15-2L-25-1	861.51	8.77	47.74	3.08	0.058	5.19	24.58	2.56	

Note: P = axial force, δ = axial deformation, f_{co} = unconfined stress, f_{cc} = confined stress, f_{cc}/f_{co} = normalised stress, ϵ_{cc} = axial strain, $\epsilon_{cc}/\epsilon_{co}$ = normalised strain, f_{ie} = effective confinement pressure, ρ_v = effective volumetric confinement ratio.